Journal of Metals, Materials and Minerals, Vol. 30, No. 4, pp. 45-50, 2020

The usage of CoAl–layered double oxide for removal of toxic dye from aqueous solution

Pornnapa TONGCHOO[1], Sonchai INTACHAI[1,*], Prakaidao PANKAM[2], Chomponoot SUPPASO[2], and Nithima KHAORAPAPONG[2]

[1] *Department of Chemistry, Faculty of Science, Thaksin University, Phatthalung, 93210, Thailand*
[2] *Department of Chemistry, Faculty of Science, Khon Kaen University, Khon Kaen 40002, Thailand*

***Corresponding author e-mail:** sonchai.i@tsu.ac.th

Received date:
5 July 2020
Revised date
28 October 2020
Accepted date:
31 October 2020

Keywords:
Layered double oxide;
Orange II;
Methyl orange;
Phenolphthalein;
Methylene blue

Abstract

CoAl−layered double oxide derived from calcination of CoAl−layered double hydroxide at 400 °C for 120 min, delivered the change in microstructure with increasing surface area. Spinel Co_3O_4 was the majority in the product as confirmed by X-ray diffraction, and Fourier transform infrared and UV-visible spectroscopies. The calcined product, CoAl−layered double oxide resulted in significant adsorption capacity on dye removal superior to that of CoAl−layered double hydroxide. The adsorbed amounts of the diverse dyes increased as follows: methylene blue < phenolphthalein < methyl orange < orange II. The adsorption affinity between adsorbent and dyes relied on electrostatic interaction and physical adsorption.

1. Introduction

Nowadays, the quality of natural water resources is numerously degenerative. One of the possibilities may be arisen from contaminating chemical effluents including textile dyes [1]. Generally, not all places have effective ways of cleaning the water from the dyeing process before discharging into the environment. Some dyes cannot be naturally degraded, meanwhile, others are degraded by producing harmful species more. Menacingly, some dyes can be carcinogenic, genotoxic and so on, even a tiny amount of the dyes enters the body [2]. The toxicity of textile dyes including methylene blue, rhodamine B, eriochrome black T, phenolphthalein, methyl orange, orange II and so on has been studied so far [1-4]. Considering the adverse effect on environment and health of people due to rapidly growing dye industries, it is important to make an effort to reduce dye pollution. Different techniques such as photocatalysis [5], biological treatment [6], and membrane separation [7] have been used in the removal of dyes from aqueous solutions, typically, adsorption of dyes onto solid adsorbents is an effective and practical way because a solid adsorbent is chemical resistant and can be reusable [8].

Layered double oxide (LDO) is an inorganic solid, which is simply conducted by calcination of layered double hydroxide (LDH). Many interesting aspects of LDO materials are large surface area, high performance on reusability, chemical, and thermal stability [8]. There is a variety of LDHs with different types of metal ions including CoAl−LDH, NiAl−LDH, NiFe−LDH, CoFe−LDH, and ZnCr−LDH used as LDO precursors [7,9,10]. Among all of them, CoAl−LDH has been intensively used to perform effective LDO, which promoted great advantages for catalysts, catalyst support, adsorbent, and so on [11-13]. The usage of LDO on the adsorptive removal of various dyes is worth investigation.

In this study, the adsorption of four organic dyes including methyl orange, orange II, methylene blue, and phenolphthalein on CoAl−LDO surface was carried out. Several adsorbents such as activated carbon, carbon nanotube, and zeolite have been explored for the adsorption of organic dyes [14-16]. Among all of them, LDO is one of the widely used adsorbents due to the large surface area, ion exchanged and adsorbed properties. CoAl−LDO has been used as an adsorbent for the removal of eriochrome black T [13]. Many works also reported advantages of CoAl−LDO for removal of other dyes [12,14], however, there is no experimental study proved that the adsorption interaction between CoAl−LDO and dyes is an important role for the removal of dyes from solutions. Herein, the comparative study of the adsorption of dyes with different charges and molecular structures, including, methyl orange and orange II (negative charge, methylene blue (positive charge, and phenolphthalein (neutral molecule) on CoAl−LDO surface was investigated. The electrostatic interaction, physical adsorption, and/or molecular size took place in the adsorption process.

2. Experimental

2.1 Materials

Chloride salts of aluminium ($AlCl_3 \cdot 6H_2O$) and cobalt ($CoCl_2$) were obtained by Carlo Erba Reagenti. Urea ($(NH_2)_2CO$) was purchased from Asia Pacific Specialty Chemicals LTD. All the dyes, including

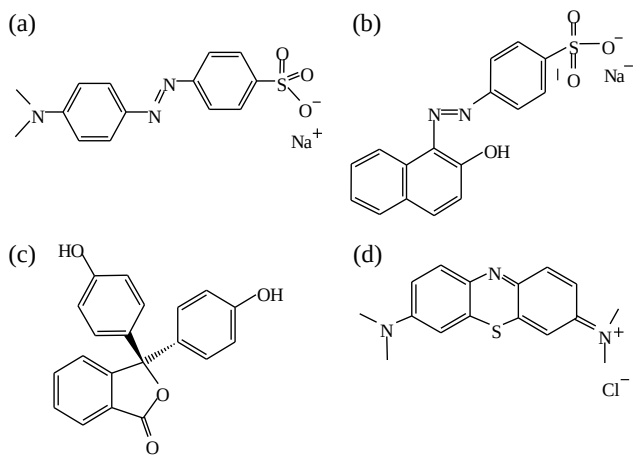

Scheme 1. The molecular structure of (a) methyl orange, (b) orange II, (c) phenolphthalein and (d) methylene blue.

methyl orange ($C_{14}H_{14}N_3NaO_3S$), orange II ($C_{16}H_{11}N_2NaO_4S$), methylene blue ($C_{16}H_{18}ClN_3S$), and phenolphthalein ($C_{20}H_{14}O_4$), from Acros, were used as the representative pollutants. Their molecular structures are displayed in Scheme 1. All chemicals are reagent grade and were used directly without any further purification.

2.2 Preparation of CoAl−LDO

CoAl−LDH, a CoAl−LDO precursor, was conducted by refluxing the mixture of the aqueous solutions of $CoCl_2$, $AlCl_3$, and $(NH_2)_2CO$ under magnetic stirring at 97°C in N_2 atmosphere for 48 h. The reaction was set up in a two-necked round-bottom flask that equipped with a reflux condenser. CoAl−LDH precipitate was collected by centrifugation, washed many times with deionized (DI) water and then ethanol, and dried at 60°C to obtain CoAl−LDH solid. After that, the as-prepared CoAl−LDH powder was calcined at 400°C for 120 min for altering layered double hydroxide to layered double oxide. The calcined product was obtained and abbreviated as CoAl−LDO.

2.3 Migration of dye from solution

The adsorption ability of CoAl−LDO was investigated by the removal of dye from solution at room temperature in the dark region. Firstly, the aqueous solution with 20 ppm concentration of methyl orange, orange II, or methylene blue was prepared by dissolving the appropriate amount of each dye powder in deionized (DI) water. On the other hand, phenolphthalein powder was dissolved in the mixed solution of 1:1%v/v of DI water and ethanol, then 100 mL of each dye solution was poured into a beaker. Secondly, 15 mg of the adsorbent (CoAl−LDO or CoAl−LDH) was mixed in the 100 mL of the dye solution (20 ppm) under magnetic stirring for 3 h. Finally, the supernatant was collected at 5, 10, 20, 30, 45, 60, 90, 120, 150, and 180 min to measure the absorbance using UV-visible spectrophotometer. The concentration of dye solution at different reaction time was determined using the relationship between the resulting absorbance and calibration curve. The removal efficiency and adsorption capacity were calculated as follows:

$$Removal\ efficiency\ (\%) = [(C_0 - C_t)/C_0] \times 100 \quad (1)$$

$$Adsorption\ capacity,\ q_e\ (mg \cdot g^{-1}) = [(C_0 - C_e)/m] \times V \quad (2)$$

Where "C_0, C_t and C_e" are the concentration ($mg \cdot L^{-1}$) of dye at the initial time (C_0), different "t" time (min) (C_t) and equilibrium (C_e), q_e ($mg \cdot g^{-1}$) is adsorption capacity at equilibrium, m (g) is the mass of adsorbent, V (L) is the volume of dye solution.

2.4 Characterization

Powder X-ray diffraction (XRD) patterns were collected on a Bruker D8 ADVANCE diffractometer using monochromatic CuKα radiation (α = 1.5418 Å). Fourier transformed infrared (FTIR) spectra of the powder samples were recorded on a Perkin Elmer Spectrum One FT-IR spectrophotometer by KBr disk method. Scanning electron microscope (SEM) images were measured on a LEO-1450VP. Nitrogen adsorption/desorption isotherms were obtained on a Micromeritics ASAP 2010 equipment, after the sample was degassed at 120°C under vacuum for 3 h. Diffuse reflectance absorption spectra of the products were recorded on a Shimadzu UV-VIS-NIR 3101PC spectrophotometer in the range of 200-800 nm using an integrated sphere. UV-visible absorption spectra of the unadsorbed dye were conducted in the wavelength range of 200-800 nm using a Shimadzu UV-1700 Pharmaspec UV-VIS spectrophotometer.

3. Results and discussion

3.1 Characterization of the inorganic adsorbent

The XRD patterns of the as-prepared CoAl−LDH and its calcined product are displayed in Figure 1. The XRD pattern of CoAl−LDH revealed a (003) characteristic plane of LDH structure at 2theta = 11.7° [7,17]. After calcination at 400°C for 2 h, the (003) reflection due to LDH was dismissed. This might be due to the transformation of LDH to be LDO, however, the small amount of LDH might be contained in the product and could not be detected by the XRD technique.

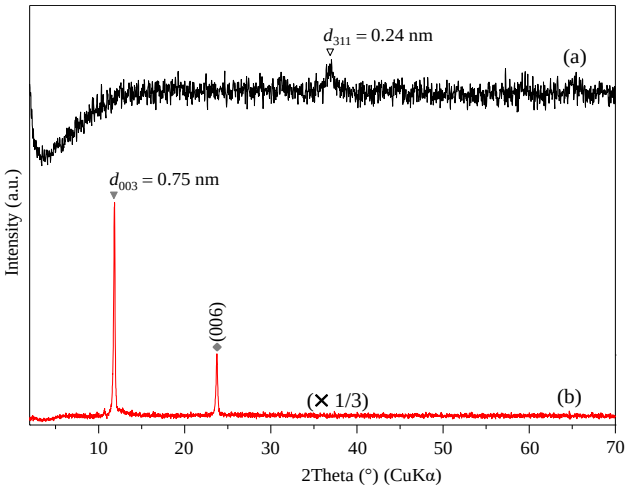

Figure 1. XRD patterns of (a) CoAl−LDO and (b) CoAl−LDH.

Meanwhile, the new diffraction peak at 36.9° corresponding to the interplanar spacing (d) of 0.24 nm was observed (Figure 1(a)). It was reported that the XRD pattern of Co_3O_4 showed the diffraction peaks at 2theta position of 31.3°, 36.9°, 59.5° and 65.4° corresponding to (220), (311), (511) and (440) planes, respectively [18]. A diffraction peak of Co_3O_4 coated with silica was also observed at 36.9° that matched (311) reflection [19]. In addition, no peak due to other aluminium compounds such as Al_2O_3 and/or $AlCo_2O_4$ was observed on the XRD pattern of CoAl−LDO that might be due to the formation of a small amount and/or low crystalline size of the compounds contained in the calcined product. As a result, it could indicate that the spinel Co_3O_4 was mostly presented in the calcined product.

The Fourier transform infrared (FTIR) spectra of both samples are shown in Figure 2, the FTIR spectrum of CoAl−LDH revealed a characteristic band at 1357 and 790 cm^{-1} due to carbonate anion [7], confirming the formation of CoAl−LDH with carbonate anion in the interlayer space. The bands at 627 and 427 cm^{-1} were attribute to the vibrations of Co–O and/or Al–O vibrations in LDH. A very broad band at 3437 cm^{-1} was due to O−H stretching of the hydroxide layer and water molecules [7]. The band at 1632 cm^{-1} could be ascribed to O−H bending of the hydroxide layer and the deformation vibration of the intercalated water molecules. This data supported the successful preparation of LDH. After the calcination (Figure 2(a)), the weak bands due to O−H stretching (3437 cm^{-1}) and O−H bending (1632 cm^{-1}) vibrations still remained in the spectrum of CoAl−LDO (Figure 2(b)). On the other hand, the characteristic band due to carbonate anion dismissed and the other absorption bands at 674 and 558 cm^{-1} corresponded to spinel Co_3O_4 were seen [19,20]. This result could further confirm the formation of CoAl−LDO together with spinel Co_3O_4.

After the calcination, the color of CoAl−LDH (magenta, Figure 3(a)) changed to black (Figure 3(b)), indicating the change in the component and/or microstructure of the product. The morphology of CoAl−LDH and CoAl−LDO was further characterized by scanning electronic microscopy. The hexagonal plate-shaped crystals with an average lateral size of 132 nm were seen in the SEM image of CoAl−LDH (Figure 3(c)) together with the large crystals due to aggregation of several platelets [13]. The morphology change was mostly observed in the image of CoAl−LDO, while a small amount of hexagonal plates also appeared in the calcined product. As a result of the calcination, the most hexagonal morphology of CoAl−LDH was thought to be uniformly delaminated and restructured to form LDO as shown in Scheme 2.

The nitrogen adsorption-desorption isotherm of CoAl−LDO and CoAl−LDH was Type IV (not shown). Meanwhile, the hysteresis loop of the adsorption isotherm was classified as Type H3 loop that corresponded to the aggregation of plate-like particles, associating with slit-shaped pores. This indicated the characteristic of typical mesoporous adsorbents [21]. An increase of the BET surface area was observed from CoAl−LDH (13 $m^2 \cdot g^{-1}$) to CoAl−LDO (176 $m^2 \cdot g^{-1}$) (Table 1). CoAl−LDO gave the average pore diameter of 7.1 nm and the maximum pore size distribution of 2.2 nm, which were decreased compared with those of CoAl−LDH (28.6 and 2.4 nm), implying that the disordered attachment among several nanosheets blocked some pores, resulting in the large number of exposed surface active sites (Scheme 2). This result might increase the adsorption property of CoAl−LDO mentioned below.

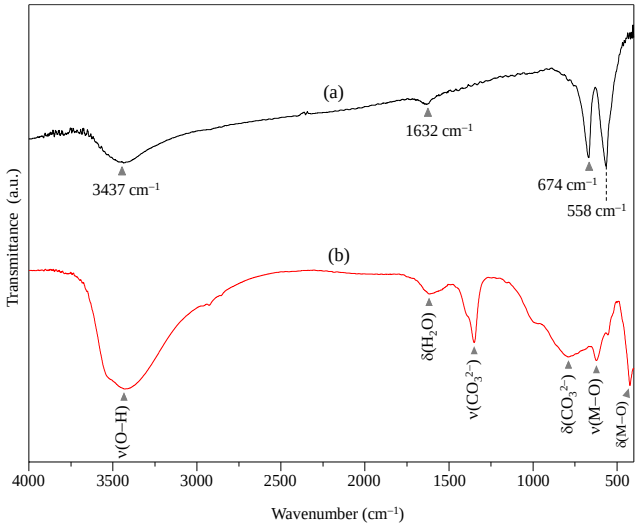

Figure 2. FTIR spectra of (a) CoAl−LDO and (b) CoAl−LDH.

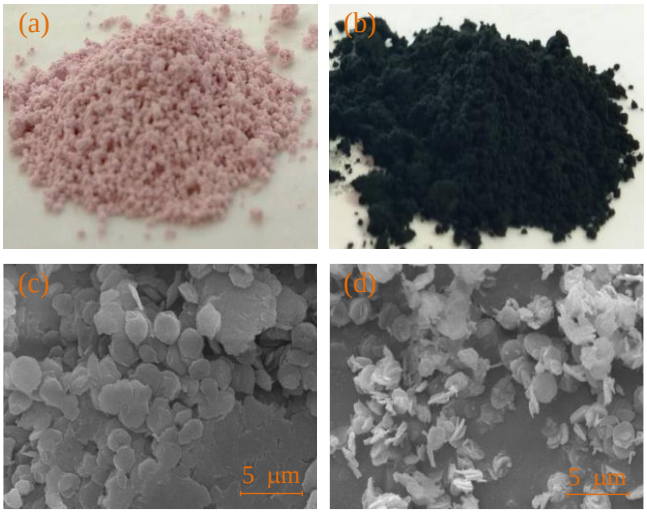

Figure 3. Colors and SEM images of (a, c) CoAl−LDH and (b, d) CoAl−LDO.

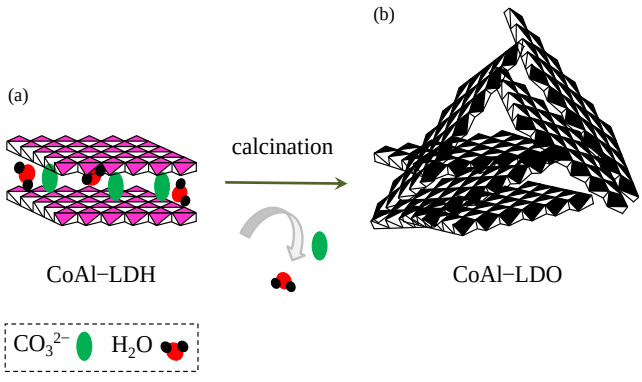

Scheme 2. Possible arrangement of CoAl−LDO derived from CoAl−LDH by calcination.

Table 1. Surface area, dye removal efficiency and equilibrium adsorption capacity of the adsorbents.

Product	Surface area	Dye removal efficiency (%)/Equilibrium adsorption capacity (mg·g^{-1})			
	(m^2·g^{-1})	methyl orange	orange II	phenolphthalein	methylene blue
CoAl−LDO	178	73/97.3	100/133.3	17/22.6	14/18.6
CoAl−LDH	13	52/69.3	73/97.3	6/8.0	4/5.3

The UV-visible spectrum of CoAl−LDH showed a shoulder at 250 nm, and the weak and/or broad bands centered at 457, 495, 528, and 621 nm (Figure 4(b)). The absorption band and shoulder at 250 and 457 nm was due to ligand-to metal charge-transfer (LMCT) from 2p orbital of oxygen to 3d orbital Al ($O_{2p} \rightarrow Al_{3d}$) and to 3d orbital of Co^{2+} ($O_{2p} \rightarrow Co_{3d}$), respectively. The broad absorption band in the range of 470 to 700 nm of the as-prepared CoAl−LDH resembled the three d-d electronics transitions of $^4T_{1g}(F) \rightarrow {}^4T_{1g}(P)$ (495 nm), $^4T_{1g}(F) \rightarrow {}^4A_{2g}$ (528 nm) and $^4T_{1g}(F) \rightarrow {}^4T_{2g}$ (621 nm) of Co^{2+} that coordinated with weak ligands in the octahedral field [10]. The broad and strong bands that appeared at 400 and 643 nm for CoAl−LDO might be due to the formation of Co^{3+} (Co_3O_4 and/or a small amount of $AlCo_2O_4$) species (Figure 4(a)). The increase of the light absorption intensities and the shift of the bands into the visible light region might arise from a topotactic phase transition including surface defects in CoAl−LDO.

3.2 Dye removal ability of the adsorbents

The adsorption ability of CoAl−LDO and CoAl−LDH was evaluated by removal of the dyes from aqueous solution as shown in Figure 5 and Figure 6. Clearly seen in Figure 5, the adsorption capacity of CoAl−LDO for whole dyes was higher than that of CoAl−LDH, the result was thought because of the large surface area (Table 1). The amounts of the dyes adsorbed on the adsorbent surfaces was increased as increasing the contact time (Figure 6), whereas the removal rate was fast at the initial time and reached the adsorption equilibrium at 45 min. As a result, the dye removal ability of the adsorbents was dependent on the charge and structure of the pollutants where it increased as follows: methylene blue (cationic dye) < phenolphthalein (neutral dye) < methyl orange, and orange II (anionic dyes). The result corresponded to the adsorption capacity of CoAl−LDO and CoAl−LDH that listed in Table 1. The main reason was due to the electrostatic interaction between positive layered charge of the adsorbent (CoAl−LDO) and negative charge of anionic dyes (methyl orange and orange II), as well as the physical adsorption [13,17]. The larger amounts of neutral dye were captured on the adsorbent surface than that of the cationic dye that arisen from the hydrophobic interaction and hydrogen bonding (for phenolphthalein), meanwhile, the electrostatic repulsion took place between methylene blue and positively charged surface of CoAl−LDO. Considering two anionic dyes, the adsorption of methyl orange and orange II on CoAl−LDO surface was varied as a result of the difference in their size and shape. The adsorption of orange II on CoAl−LDO surface (q_e = 133.3 mg/g) was better than that of methyl orange (q_e = 97.3 mg/g) because of the larger number of capturing sites including two aromatic rings on the hydrophobic tail of orange II, and two hydrogen bonding sites on two lone pairs of oxygen atom (Scheme 1) that promoted more active sites to interact with the adsorbents [8]. As we have known, the comparative study on the adsorption between different charge and size (the number of aromatic rings and hydrogen bonding sites) of dye on CoAl−LDO surface was not reported [13-14]. The present work showed that the usage of CoAl−LDO as positively charged adsorbent was an advantage on the adsorption of anionic dyes especially possessing more aromatic ring and hydrogen bonding sites in the structure. Furthermore, CoAl−LDO possessed higher capacity on the removal of orange II than those of polyaniline/bentonite [24], surfactant/zeolite [25] and cationic surfactant/palygorskite [26] used as the adsorbent. Because there is the contamination of different dyes on charge and size in natural water, this study showed the versatile interactions for

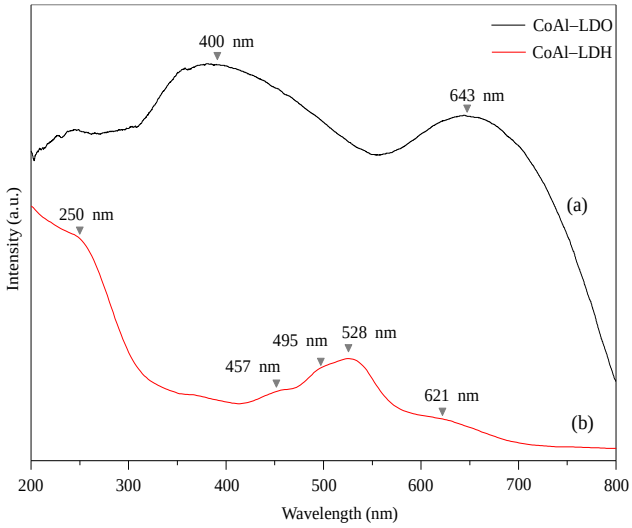

Figure 4. UV-visible absorption spectra of (a) CoAl−LDO and (b) CoAl−LDH.

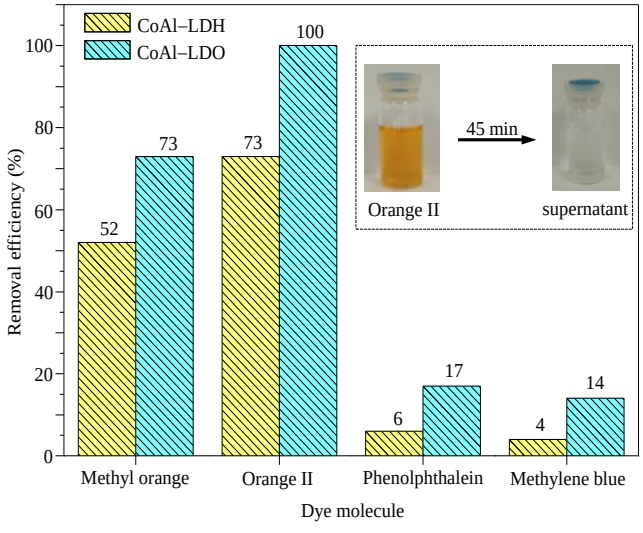

Figure 5. Removal efficiency of CoAl−LDO and CoAl−LDH on various dyes.

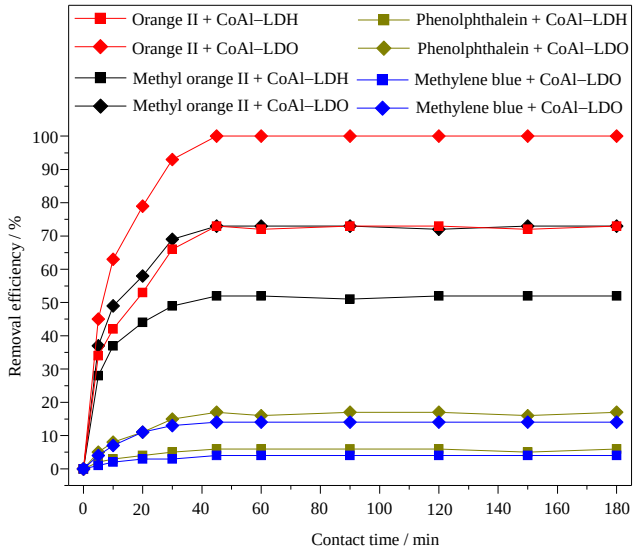

Figure 6. Effect of contact time on dye removal efficiency of CoAl–LDO and CoAl–LDH.

the considerable purification of wastewater on CoAl–LDO surface. The selection of suitable dyes and inorganic solids based the electrostatic interaction should be considered for an effective adsorption process. Besides, the developing smart adsorbent containing multifunctionality for the adsorption of various dye mixture with different charge and size together with the magnetic feature to support the separation of solid particles on the reusability should be further investigated.

4. Conclusions

CoAl–layered double oxide was prepared via calcination of pristine CoAl–layered double hydroxide at 400°C for 2 h. The surface area of the calcined products increased from 13 to 178 $m^2 \cdot g^{-1}$. The anionic dyes, orange II and methyl orange, were mostly removed from the solutions as a result of the electrostatic interaction between CoAl–layered double oxide and the dyes. Meanwhile, the physical adsorption of phenolphthalein and methylene blue on the surface of the adsorbents was due to hydrophobic interaction and hydrogen bonding, as well as electrostatic repulsion. The larger surface area was an important role in the adsorption ability of CoAl–LDO compared with CoAl–LDH.

Acknowledgements

This work was supported by Thaksin University Research Fund, Thailand. We acknowledged the Department of Chemistry, Faculty of Science, Thaksin University, for providing materials, equipment, and facilities.

References

[1] C.R. Holkar, A.J. Jadhav, D.V. Pinjari, N.M. Mahamuni, and A.B. Pandit, "A critical review on textile wastewater treatments: Possible approaches," *Journal of Environmental Management*, vol. 182, pp. 351-366, 2016.

[2] A. Tkaczyk, K. Mitrowska, and A. Posyniak, "Synthetic organic dyes as contaminants of the aquatic environment and theirimplications for ecosystems: A review," *Science of The Total Environment*, vol. 717, pp. 137222, 2020.

[3] S.S. Auerbach, D.W. Bristol, J.C. Peckham, G.S. Travlos, C.D. Hébert, and R.S. Chhabra, "Toxicity and carcinogenicity studies of methylene blue trihydrate in F344N rats and B6C3F1 mice," *Food and Chemical Toxicology*, vol. 48, pp. 169-177, 2010.

[4] D.D. Dietz, M.R. Elwell, R.E. Chapin, M.D. Shelb, M.B. Thompson, R. Filler, and M.A. Stedham, "Subchonic (13-week) toxicity studies of oral phenolphthalein in Fischer 344 rats and $B_6C_3F_1$ mice," *Fundamental and Applied Toxicology*, vol. 18, pp. 48-58, 1992.

[5] N. Khumchoo, N. Khaorapapong, A. Ontam, S. Intachai, and M. Ogawa, "Efficient photodegradation of organics in acidic solution by ZnO-smectite hybrids," *European Journal of Inorganic Chemistry*, vol. 19, pp. 3157-3162, 2016.

[6] T.R. Waghmode, M.B. Kurade, R.T. Sapkal, C.H. Bhosale, B-H. Jeon, and S.P. Govindwar, "Sequential photocatalysis and biological treatment for the enhanced degradation of the persistent azo dye methyl red," *Journal of Hazardous Materials*, vol. 371, pp. 115-122, 2019.

[7] Y. Liu, F. Zhang, W. Zhu, D. Su, Z. Sang, X. Yan, S. Li, J. Liang, and S.X. Dou, "A multifunctional hierarchical porous SiO_2/GO membrane for high efficiency oil/water separation and dye removal," *Carbon*, vol. 160, pp. 88-97, 2020.

[8] M. Zubair, M. Daud, G. McKay, F. Shehzad, and M.A. Al-Harthi, "Recent progress in layered double hydroxides (LDH)-containing hybrids as adsorbents for water remediation," *Applied Clay Science*, vol. 143, pp. 279-292, 2017.

[9] Z. Liu, R. Ma, M. Osada, N. Iyi, Y. Ebina, K. Takada, and T. Sasaki, "Synthesis, anion exchange, and delamination of Co-Al layered double hydroxide: Assembly of the exfoliated nanosheet/polyanion composite films and magneto-optical studies," *Journal of the American Chemical Society*, vol. 128, pp. 4872-4880, 2006.

[10] R. Yang, Y. Gao, J. Wang, and Q. Wang, "Layered double hydroxide (LDH) derived catalysts for simultaneous catalytic removal of soot and NO_x," *Dalton Transactions*, vol. 43, pp. 10317-10327, 2014.

[11] S. Kumar, M.A. Isaacs, R. Trofimovaite, L. Durndell, C.M.A. Parlett, R.E. Douthwaite, B. Coulson, M.C.R. Cockett, K. Wilson, and A.F. Lee, "P25@CoAl layered double hydroxide heterojunction nanocomposites for CO_2 photocatalytic reduction," *Applied Catalysis B: Environmental*, vol. 209, pp. 394-404, 2017.

[12] Z. Tian, Q. Li, J. Hou, L. Pei, Y. Li, and S. Ai, "Platinum nanocrystals supported on CoAl mixed metal oxide nanosheets derived from layered double hydroxides as catalysts for selective hydrogenation of cinnamaldehyde," *Journal of Catalysis*, vol. 331, pp. 193-202, 2015.

[13] M. Zubair, N. Jarrah, S.A. Manzar, M. AlHarthi, M. Daud, N.D. Mu'azu, and S.A. Haladu, "Adsorption of eriochrome black T from aqueous phase on MgAl-, CoAl- and NiFe- calcined layered double hydroxides Kinetic, equilibrium and thermodynamic studies," *Journal of Molecular Liquids*, vol. 230, pp. 344-352, 2017.

[14] F. Khodam, H.R. Amani-Ghadim, S. Aber, A.R. Amani-Ghadimd, and I. Ahadzadeh, "Neodymium doped mixed metal oxide derived from CoAl-layered double hydroxide: Considerable enhancement in visible light photocatalytic activity," *Journal of Industrial and Engineering Chemistry*, vol. 68, pp. 311-324, 2018.

[15] G.V. Brião, S.L. Jahn, E.L. Foletto, and G.L. Dotto, "Highly efficient and reusable mesoporous zeolite synthetized from a biopolymer for cationic dyes adsorption," *Colloids and Surfaces A: Physicochemical and Engineering Aspects*, vol. 556, pp. 43-50, 2018.

[16] M. Hasanzadeh, A. Simchi, and H. Shahriyari Far, "Nanoporous composites of activated carbon-metal organic frameworks for organic dye adsorption: Synthesis, adsorption mechanism and kinetics studies," *Journal of Industrial and Engineering Chemistry*, vol. 81, pp. 405-414, 2020.

[17] O.A. Shabaan, H.S. Jahin, and G.G. Mohamed, "Removal of anionic and cationic dyes from wastewater by adsorption using multiwall carbon nanotubes," *Arabian Journal of Chemistry*, vol. 13, pp. 4797-4810, 2020.

[18] Y. Chen, C. Jing, X. Zhang, D. Jiang, X. Liu, B. Dong, L. Feng, S. Li, and Y. Zhang, "Acid-salt treated CoAl layered double hydroxide nanosheets with enhanced adsorption capacity of methyl orange dye," *Journal of Colloid and Interface Science*, vol. 548, pp. 100-109, 2019.

[19] C. Feng, J. Zhang, Y. Deng, C. Zhong, L. Liu, and W. Hu, "One-pot fabrication of Co_3O_4 microspheres via hydrothermal method at low temperature for high capacity supercapacitor," *Materials Science and Engineering: B*, vol. 199, pp. 15-21, 2015.

[20] J. Gamonchuang, N. Khaorapapong, and M. Ogawa, "The effect of alcohol type on the thickness of silica layer of Co_3O_4@ SiO_2 core-shell particle," *Colloids and Surfaces A: Physicochemical and Engineering Aspects*, vol. 511, pp. 39-46, 2016.

[21] M. Salavati-Niasari, N. Mir, and F. Davar, "Synthesis and characterization of Co_3O_4 nanorods by thermal decomposition of cobalt oxalate," *Journal of Physics and Chemistry of Solids*, vol. 70, pp. 847-852, 2009.

[22] K.S.W. Sing, and R.T. Williams, "Physisorption hysteresis loops and the characterization of nanoporous materials," *Adsorption Science and Technology*, vol. 22, pp. 773-782, 2004.

[23] Y. Qiu, B. Lin, F. Jia, Y. Chen, B. Gao, and P. Liu, "CdS-pillared CoAl-layered double hydroxide nanosheets with superior photocatalytic activity," *Materials Research Bulletin*, vol. 72, pp. 235-240, 2015.

[24] W. Li, Q. Lin, M. Gao, and H. Ma, "Adsorption studies of Orange II onto polyaniline/bentonite nanocomposite," *Water Science and Technology*, vol 76, pp. 337-354, 2017.

[25] X. Jin, B. Yu, Z. Chen, J. M. Arocena, and R. W. Thring, "Adsorption of orange II dye in aqueous solution onto surfactant-coated zeolite: Characterization, kinetic and thermodynamic studies," *Journal of Colloid and Interface Science*, 435, pp. 15-20, 2014.

[26] B. Sarkar, Y. Xi, M. Megharaj, and R. Naidu, "Orange II adsorption on palygorskites modified with alkyl trimethylammonium and dialkyl dimethylammonium bromide - An isothermal and kinetic study," *Applied Clay Science*, vol. 51, pp. 370-374, 2011.